Leggett-Garg tests of macrorealism for bosonic systems including double-well Bose-Einstein condensates and atom interferometers

L. Rosales-Zárate, B. Opanchuk, Q. Y. He, and M. D. Reid

Phys. Rev. A **97**, 042114 — Published 19 April 2018

DOI: 10.1103/PhysRevA.97.042114

Leggett-Garg tests of macro-realism for bosonic systems including double-well Bose-Einstein condensates and atom interferometers

L. Rosales-Zárate[1,2], B. Opanchuk[1], Q. Y. He[3] and M. D. Reid[1]
[1] *Centre for Quantum and Optical Science, Swinburne University of Technology, Melbourne 3122 Australia*
[2] *Centro de Investigaciones en Óptica A.C., León, Guanajuato 37150, México and*
[3] *State Key Laboratory of Mesoscopic Physics, School of Physics, Peking University, Beijing 100871 China*

We construct quantifiable generalisations of Leggett-Garg tests for macro/ mesoscopic realism and noninvasive measurability that apply when not all outcomes of measurement can be identified as arising from one of two macroscopically distinguishable states. We show how quantum mechanics predicts a negation of the LG premises for strategies involving ideal-negative-result, weak and quantum non-demolition measurements on dynamical entangled systems, as might be realised with Bose-Einstein condensates in a double-well potential, path-entangled NOON states and atom interferometers. Potential loopholes associated with each strategy are discussed.

I. INTRODUCTION

In his paradox where a cat is apparently both dead and alive, Schrodinger raised the possibility of an inconsistency between macroscopic realism and quantum mechanics [1]. Leggett and Garg (LG) suggested to test macroscopic realism by comparing the predictions of quantum mechanics with those based on two classical premises [2]. The first premise is *macroscopic realism per se* (MRPS): a macroscopic system with two macroscopically distinguishable states available to it will at all times be in one or other of these states. The second premise is *macroscopic noninvasive measurability* (NIM): for such a system, it is possible, in principle, to determine which of these states the system is in, with arbitrarily small perturbation on the subsequent dynamics.

Leggett and Garg showed how the two premises (referred to as macro-realism) constrain the dynamics of a two-state system. Considering three successive times $t_3 > t_2 > t_1$, the variable S_i denotes which of the two states the system is in at time t_i, the respective states being denoted by $S_i = +1$ or -1. The Leggett-Garg premises imply the LG inequality [2, 3]

$$LG \equiv \langle S_1 S_2\rangle + \langle S_2 S_3\rangle - \langle S_1 S_3\rangle \leq 1 \qquad (1)$$

More recent work shows how the LG premises also imply the "no disturbance" or "no signalling in time" condition [4, 5]

$$d_\sigma \equiv \langle S_3|\hat{M}_2,\sigma\rangle - \langle S_3|\sigma\rangle = 0 \qquad (2)$$

Here $\langle S_3|\hat{M}_2,\sigma\rangle$ (and $\langle S_3|\sigma\rangle$) is the expectation value of S_3 given that a measurement $\hat{M}_2$ is performed (or not performed) at time t_2, conditional on the system being prepared in a state denoted σ at time t_1. The LG inequality and no-disturbance conditions are predicted to be violated for many quantum systems where the dynamics involves the formation of quantum superposition states [2–17]. The work of Leggett and Garg represented an advance, since it extended beyond the quantum framework to show how the macroscopic quantum superposition state defies classical macroscopic reality.

The Leggett-Garg approach raised new ideas about how to test quantum mechanics even at the microscopic level [6, 8–11]. Failure of the inequalities implies no classical trajectory exists between successive measurements: either the system cannot be viewed as being in a definite state independent of observation, or there cannot be a way to determine that state, without interference by the measurement. Noninvasive measurability is "vexing" to justify, however, because of the plausibility of the measurement disturbing the system. Leggett and Garg countered this problem by proposing an ideal negative result measurement (INR): the argument is conditional on the first postulate being true e.g. *if* a photon does travel through one slit *or* the other, a null detection beyond one slit is justified to be noninvasive [2, 9, 10, 14]. A second approach is to perform weak measurements [18–21] that enable calculation of the moment $\langle S_2 S_3\rangle$ in a limit where there is a vanishing disturbance to the system [11–13, 20, 22]. A third approach is to test modified LG inequalities that quantify the invasiveness of "clumsy" quantum nondemolition (QND) measurements [4, 17, 23]. So far, experimental investigations have mainly focused on superconducting circuits or small systems (e.g. single atoms or photons). Recent developments include theoretical proposals for mechanical oscillators [16] and macroscopic states of atoms [17].

An illuminating Leggett-Garg test would be for a mesoscopic massive system in a quantum superposition of being at two different locations [24]. As of yet, there has to our knowledge been no LG test involving a mesoscopic system (of several particles or more) that is at time t_2 in a quantum superposition of being at two different locations. An example of such a superposition is the path-entangled NOON state, written as $|\psi\rangle = \frac{1}{\sqrt{2}}\{|N\rangle_a|0\rangle_b + |0\rangle_a|N\rangle_b\}$ where $|N\rangle_{a/b}$ is the N-particle state for two spatially separated modes a (b) [25–27]. In this case the ideal negative result measurement can be applied, and justified as noninvasive by the assumption of Bell's locality [28]. For massive systems, this is especially interesting [24]. A method is then given to negate that the system must be located either "here" or "there", or else to conclude there is a disturbance to a massive

system due to a measurement performed on a vacuum at a different location.

In this paper, we show how such tests may be possible on a mesoscopic scale. As one example, in Sections II and III, we show that violations of Leggett-Garg inequalities are predicted for Bose-Einstein condensates (BEC) trapped in two separated potential wells of an optical lattice. Here dynamical oscillation of large groups of atoms to form NOON macroscopic superposition states is predicted at high nonlinearities [29–35]. To date, there has been no LG test based on matter-wave interference with Bose-Einstein condensates, despite that these systems exhibit entanglement [36–43], have demonstrated Josephson oscillation [29] and are likely candidates for mesoscopic superpositions of states with a distinct centre of mass [31].

A problem however for an experimental realisation is the fragility of the macroscopic superpositions. Under specific conditions, NOON states can be generated, allowing an INR strategy. Otherwise, for less fragile macroscopic superposition states, we derive in Section IV *modified s-scopic LG inequalities* that can be used to test LG premises for superpositions of the type $|\psi\rangle = \frac{1}{\sqrt{2}}\{|N-n\rangle_a|n\rangle_b + |n\rangle_a|N-n\rangle_b\}$ $(n < N)$. These superpositions deviate from the ideal NOON superposition by allowing mode population differences not equal to $-N$ or N. The modified LG inequalities are thus useful where outcomes are not always constrained to being "dead" or "alive", and allow a quantification of the degree of realism that is being tested. In the proposals of this paper, the relevant measure of macroscopicity is the mass difference given by sm_A (in each mode) of the two states forming the superposition, m_A being the mass of each atom.

The ideal negative result measurement may be difficult to apply where there are residual atoms in both modes, and we thus develop (in Sections III.B and III. C) QND and weak measurement strategies for testing the Leggett-Garg premises and demonstrating mesoscopic quantum coherence in this case. This opens the way to test mesoscopic realism and demonstrate mesoscopic quantum coherence in the experiments of Albiez et al [29], that observe oscillation of the relative populations of two weakly-linked BECs across the two wells of a double-well potential created in an optical lattice and separated by $\sim 5\mu m$.

The strategies and inequalities developed in this paper are applicable to atom and photonic interferometers involving multiparticle bosonic states. In Section IV, we show how to test the Leggett-Garg premises where mesoscopic states are created at the time t_2 within the interferometer, and a subsequent measurement is made at time t_3 of the population difference after passage through the interferometer. This approach can be applied to either nonlinear atom interferometers where the bosons are subject to nonlinearity due to a medium, or to linear interferometers that use only beam splitters, conditional measurements and phase shifts. In this context, we discuss violations of the *s*-scopic Leggett–Garg in which the two premises of macroscopic realism per se (MRPS) and non-invasive measureability (NIM) are asymmetrically quantified, being specified by two different parameters s_2 and s_3.

For linear interferometers, while violation of mesoscopic LG inequalities may be difficult, it is nonetheless possible in principle to test the Leggett-Garg premises as applied to individual atomic trajectories. This provides an avenue for a Leggett-Garg test using matter waves passing through an atom interferometer, that would demonstrate the no-classical trajectories result for atoms. By exploiting different spatial separations and atomic species, such tests would complement the Leggett-Garg test of Robens et al that shows violation of a Leggett-Garg inequality for a Cesium atom performing a quantum walk, where the spread in distance of the atomic wave function is $\sim 2\mu m$ [10].

To conclude, in Section V we give a discussion of potential loopholes for each of the strategies that have been presented in this paper, as see from the perspective of a macro-realist committed to the premises of Leggett-Garg. Loopholes arise from the need to make a measurement at the time t_2 in order to evaluate the two-time correlation functions $\langle S_2 S_3\rangle$ and $\langle S_1 S_3\rangle$ correctly. For each of the three strategies, there are additional assumptions that justify that the measurement employed in the experiment will give the same correlation functions for the Leggett-Garg inequality as the non-invasive measurement (NIM) defined in the Leggett-Garg premise. These additional assumptions imply that for each strategy a somewhat different model for macro-realism is tested.

II. DYNAMICS OF A MESOSCOPIC TWO-STATE OSCILLATION

The Hamiltonian H_I for an N-atom condensate constrained to a double well potential reveals a regime of macroscopic two-state dynamics. The two-well system has been reliably modelled by the Josephson two-mode Hamiltonian [29–39, 41–44]

$$H_I = 2\kappa \hat{J}_x + g\hat{J}_z^2 \tag{3}$$

Here $\hat{J}_z = (\hat{a}^\dagger\hat{a} - \hat{b}^\dagger\hat{b})/2$, $\hat{J}_x = (\hat{a}^\dagger\hat{b} + \hat{b}^\dagger\hat{a})/2$, $\hat{J}_y = (\hat{a}^\dagger\hat{b} - \hat{b}^\dagger\hat{a})/2i$ are the Schwinger spin operators defined in terms of the boson operators $\hat{a}^\dagger, \hat{a}$ and $\hat{b}^\dagger, \hat{b}$, for the modes describing particles in each of the wells, labelled a and b respectively. The κ represents interwell hopping and g the nonlinear self-interaction due to the medium. For high interaction strength ($Ng/\kappa \gg 1$), regimes exists where a mesoscopic two-state oscillation (of period T_N) takes place (Fig. 1) [30, 33]. If the system is prepared in $|N\rangle_a|0\rangle_b$, then at a later time t' the state vector is to a good approximation (apart from a phase factor)

$$|\psi(t)\rangle = \cos(t)|N\rangle|0\rangle + i\sin(t)|0\rangle|N\rangle \tag{4}$$

where $t = E_\Delta t'/\hbar$ and E_Δ is the energy splitting of the energy eigenstates $|N\rangle|0\rangle \pm |0\rangle|N\rangle$ under H_I. In one state,

$|N\rangle_a|0\rangle_b$, all N atoms are in the well a and in the second state, $|0\rangle_a|N\rangle_b$, all atoms are in the well b [33]. The interaction H_I also describes Josephson effects in superconductors [45], superfluids [46] and exciton polaritons [47].

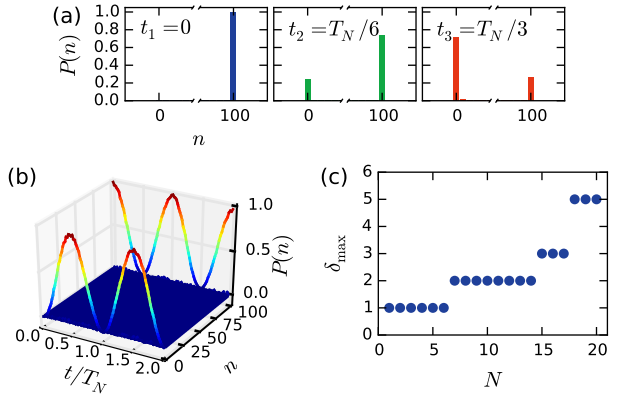

Figure 1. *Two-state NOON dynamics*: (a) The probability $P(n)$ of n atoms in well a at times 0, $T_N/6$, $T_N/3$. Here $N = 100$, $g = 1$. T_N is the two-state oscillation period. The system undergoes oscillation between two states, where all atoms are in one or other well. The probability of obtaining results other than $n = 0$ or 100 is negligible. The Leggett-Garg inequality (1) is violated with $LG = 1.5$ for states distinct by $s = 100$ atoms in each well. (b) $P(n)$ versus time t for the system described in (a). (c) An upper bound on the backaction δ due to the ideal negative result (INR) measurement that can be tolerated for an LG violation. Here δ is plotted versus N, the total number of atoms in the system.

The quantum solution (4) predicts a violation of the LG inequality [34]. Here, we denote the sign of the outcome J_z of the spin measurement $\hat{J}_z$ at time t_i by S_i ($S_i = 1$ if $J_z \geq 0$; $S_i = -1$ if $J_z < 0$). The two-time correlation $\langle S_i S_j \rangle = \cos[2(t_j - t_i)]$ is independent of the initial state, whether $|N\rangle|0\rangle$ or $|0\rangle|N\rangle$. Choosing $t_1 = 0$, $t_2 = \pi/6$, $t_3 = \pi/3$ (or $t_3 = 5\pi/12$), the quantum prediction is $LG = 1.5$ (1.37) which gives a violation of (1) [2]. We have solved the Hamiltonian (2) for $N = 100$ and $g = 1$ (Figure 1) confirming the ideal correlations that give violation of the LG inequality in this regime.

The oscillation times T_N however are impractically high for proposals based on Rb atoms [29, 33, 48]. The fragility of the macroscopic superposition state and the measured decoherence times for a BEC suggest such an experiment to be infeasible [49]. It is known however that practical oscillation times can be obtained using a different initial state $|N - n_L\rangle|n_L\rangle$ ($0 < n_L < N$), where initially there are atoms in both wells [29, 33]. The dynamical solution presented in Fig. 2 with $n_L = 10$ reveals a two-state oscillation over reduced time scales, mimicking the experiment of Albiez et al [29] for $N = 1000$ atoms where coherent oscillations were observed over milliseconds.

The objective of this paper is to propose strategies for testing LG inequalities in such experiments. There

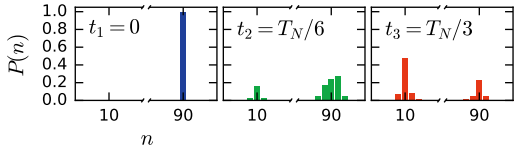

Figure 2. *Mesoscopic two-state oscillations:* Here $N = 100$, $g = 1$. The initial state has 90 atoms in mode a. The s-scopic LG inequalities (12) are violated with $LG_s = 1.2$ for $s_2 = s_3 = 80$ using a non-clumsy QND measurement $\hat{M}$ at time t_2, as described in the text.

are two questions to be addressed. The first is how to perform (or access the results of) the noninvasive measurement (NIM), assuming it exists. The second is how to test macro-realism when (as in Fig. 2) the values of S_i do not always correspond to macroscopically distinct outcomes.

III. STRATEGIES FOR ACCESSING THE RESULT OF THE NIM

The first question has been discussed quite extensively in the literature [2]. The measurement at t_1 can be made noninvasively by the preparation of a fixed number of particles in each of the modes. The $\langle S_1 S_2 \rangle$ and $\langle S_1 S_3 \rangle$ can hence be inferred using deterministic state preparation and projective measurements at t_2 and t_3, based on the LG premise that the system was in a state with definite S at time t_i, and that the projective measurement will reveal which state the system was in (and hence the value of S_i). [2]. To measure $\langle S_1 S_3 \rangle$ no intervening measurement is made at t_2, based on the assumption that the NIM at t_2 will not affect the subsequent statistics. For $\langle S_2 S_3 \rangle$, S_3 is measured projectively but the evaluation of S_2 is difficult, since with any practical measurement it could be argued that a measurement $\hat{M}$ made at t_2 is not the NIM, and does indeed influence the subsequent dynamics. Three strategies may be used to counter this objection: (1) ideal negative result (INR) measurements; (2) QND measurements; and (3) weak measurements.

A. Ideal negative result measurement (INR) strategy

A strong test is possible if the two modes of the NOON superposition (3) correspond (at time t_2) to spatially separated locations. In this case, the idea negative result (INR) strategy outlined by LG can be applied. A measurement apparatus at time t_2 couples locally to only one mode a, enabling measurement of the particle number n_a. Either $n_a = 0$ or $n_a = N$. Based on the first LG premise, if one obtains $n_a = 0$, it is assumed that there were prior to the measurement no atoms in the mode a. Hence the measurement that gives a negative result is justified to

be noninvasive. The $\langle S_2 S_3\rangle$ can be evaluated using only negative-result outcomes, as described in Leggett-Garg's original paper [2]. In such an experiment, there is implicit the assumption of locality: that there is no change to one mode because of measurement on the other.

It might be argued (based on experiments that confirm violation of Bell's inequality) that the measurement at mode a (b) *can* induce a nonlocal back-action effect on the macroscopic state of the other mode, so that there may be a change of the state of mode b (a) of up to δ particles, where $\delta \leq N$. The change δ may be microscopic, not great enough to switch the system between macroscopic states at t_2, but might alter the subsequent dynamics, to induce a macroscopic change at t_3. If we assume quantum states at t_2, then changes to the dynamics can be established within quantum mechanics, to give a range of prediction for $\langle S_2 S_3\rangle$. We have performed this calculation and plot the effect of δ for various N in Fig. 1c, noting that a moderately small backaction δ to the quantum state of one mode will destroy violations of the LG inequality even for large N.

B. Non-clumsy QND measurement strategy

A second strategy constructs a measurement $\hat{M}$ that can be shown to give a negligible disturbance to the system being measured, if it is indeed in one of the two macroscopically distinguishable states [4, 17]. This strategy is useful if the modes are co-located or both modes are occupied at t_2 (as in the experiment of [29]).

Suppose the state at time t_2 is a superposition

$$|\psi\rangle = c_-|\psi_-\rangle + c_+|\psi_+\rangle \tag{5}$$

of states $|\psi_+\rangle$ and $|\psi_-\rangle$ that give, respectively, outcomes $S = \pm 1$. Here $c_\pm$ are probability amplitudes. The first LG premise asserts that the system is in a state of either positive or negative S, at any given time. The second premise assumes there is no change to the value of S_3 at t_3, due to the noninvasive measurement (NIM) at t_2.

According to quantum mechanics, an appropriately selected QND measurement $\hat{M}$ of S will not change the state of the system at time t_2 (and hence not change the outcome at time t_3), *if* the system at time t_2 is indeed in one of the states $|\psi_+\rangle$ and $|\psi_-\rangle$ (which are eigenstates of S). Such a measurement is referred to in this paper as a "*non-clumsy*" measurement of S. The INR measurement discussed in Section III.A is an example of a non-clumsy measurement of S, for systems prepared in the NOON state. The QND strategy requires a control experiment, in order to experimentally establish that states with definite value of S are indeed unchanged by the QND measurement [4, 23]. The noninvasiveness of the measurement is then justified by the first LG premise, that the system is in a state of either positive or negative S.

In fact, for any realistic "clumsy" measurement, a small change may arise, which can be experimentally measured. One can experimentally quantify this change, if the system is indeed in one or other of the two macroscopically distinguishable states at t_2, by preparing the system in one or other state, and measuring any change to the dynamics at time t_3 as a consequence of the measurement [4, 17, 23]. Hence, the QND strategy is to measure the probabilities $P_\pm$ for the outcomes $S_2 = \pm 1$ respectively. The prediction is $P_\pm = |c_\pm|^2$. Then one prepares the system in the state $|\psi_+\rangle$ at time t_2, measuring S_3 at the later time t_3, without the measurement $\hat{M}$ being made on the state at t_2. This allows measurement of the moment $\langle S_2 S_3\rangle_+$ where the system at time t_2 is indeed in the state $|\psi_+\rangle$ at time t_2. Similarly, one prepares the system in the state $|\psi_-\rangle$ to measure $\langle S_2 S_3\rangle_-$. If the LG premises are correct, then the conclusion is that

$$\langle S_2 S_3\rangle = P_+\langle S_2 S_3\rangle_+ + P_-\langle S_2 S_3\rangle_- \tag{6}$$

and this is the same result for $\langle S_2 S_3\rangle$ that is measured using the non-clumsy measurement $\hat{M}$. The measurement of $\langle S_2 S_3\rangle$ is repeated, but this time with the measurement $\hat{M}$ being made on the prepared state $|\psi_\pm\rangle$ at the time t_2 (prior to the evolution to the later time t_3), to give a moment that we call $\langle S_2 S_3\rangle_{MC}$. If the measurement $\hat{M}$ is non-clumsy, then $\epsilon \equiv \langle S_2 S_3\rangle_{MC} - \langle S_2 S_3\rangle = 0$. A clumsy measurement can therefore change the value of LG by ϵ, but not by more than ϵ. The change due to a clumsy measurement can be quantified and thus be accounted for, through extra terms in the inequalities [4, 17, 23]. This type of experiment has been carried out recently for superconducting circuits [4]. Fig. 2 gives predictions of LG violations using such a QND measurement approach, for the two-well system.

It could be argued that this approach is limited to test a modified LG assumption, that the system is always in a *quantum* state with definite S at the time t_2. This is given the difficulty of proving that all *hidden variable states* with definite outcome of S are not changed by the QND measurement, and is related to the difficulty of preparing all such states. The individual quantum states $|\psi_\pm\rangle$, on the other hand, can be prepared accurately, and the effectiveness of preparation verified by quantum tomography. An analysis of the different models tested by the LG inequalities is given by Maroney and Timpson [50]. Regardless, if the LG inequalities are violated, the QND measurement strategy rigorously demonstrates the quantum coherence between the states $|\psi_+\rangle$ and $|\psi_-\rangle$. This is because the LG inequalities cannot be violated if the system is in, at time t_2, a probabilistic mixture of the two states $|\psi_\pm\rangle$.

We now consider a specific quantum model for such a QND measurement that applies to the two-well atomic system. The QND measurement (labelled $\hat{M}$) is modelled by the Hamiltonian

$$H_Q = \hbar G \hat{J}_z \hat{n}_c \tag{7}$$

that for atomic spin describes a measurement of $\hat{J}_z$ based on an ac Stark shift [51]. An optical "meter" field c is prepared in a coherent state $|\gamma\rangle$ and coupled to the system

for a time τ_0. The meter field is a single mode with boson operator $\hat{c}$ and number operator $\hat{n}_c = \hat{c}^\dagger \hat{c}$. The quantum model for this measurement is given in more detail in the Refs. [22, 51]. Writing the state of the atomic system at time t_2 as $\sum_{m=0}^{N} d_m |m\rangle_a |N-m\rangle_b$ (d_m are probability amplitudes), the output state immediately after measurement is (setting $\tau_0 = \pi/2NG$)

$$|\psi\rangle = \sum_{m=0}^{N} d_m |m\rangle_a |N-m\rangle_b |\gamma e^{i\pi(N-2m)/2N}\rangle_c \quad (8)$$

Homodyne detection on the optical system enables measurement of the meter quadrature phase amplitude $\hat{p} = (\hat{c} - \hat{c}^\dagger)/i$. For γ large, the different values of $\hat{J}_z$ (and hence S_2) are measurable by outcomes for $\hat{p}$ and the atomic system after the homodyne measurement collapses to a state of definite J_z. Unless the atomic system is initially in a NOON state, this is a "clumsy" measurement of S_2. The non-clumsy measurement of S_2 leaves eigenstates of S_2 (the sign of the atomic spin J_z) unchanged. The non-clumsy QND measurement thus discriminates only the sign of $\hat{p}$ and collapses the superposition state at time t_2 into one or other state, $|\psi_+\rangle$ or $|\psi_-\rangle$. For the case of Figure 2, LG violations are predicted, with γ large, for the non-clumsy measurements.

C. Weak measurement strategy

The limit $\gamma \to 0$ of the QND measurement (7) enables the weak measurement (WM) strategy [11–13, 19, 21]. Here, the *entire* quantum state of the system at t_2 is *undisturbed* by the measurement. If the system at time t_2 is in a NOON state (3) then the relation

$$\langle S_2 S_3 \rangle = -\frac{1}{2\gamma} \langle p S_3 \rangle \quad (9)$$

holds for all γ. This relation is derived in Ref. [22] and can be experimentally verified for the purpose of a LG test. Although in the weak measurement limit there is no clear resolution of the value S_2 (values can exceed the eigenvalue range [18], a phenomenon known as quantum weak values), the value of $\langle S_2 S_3 \rangle$ as given by the projective measurement can be obtained by averaging over many runs [11, 12]. The term weak measurement is here used in the sense of the measurements defined by Aharonov, Albert and Vaidmann, that yield quantum weak values [18, 20]. This contrasts with QND measurements weak in the sense that they couple only to a small part of a large system, such as coupling only to one of many modes, but nonetheless are projective measurements that collapse the system into a definite eigenstate [2, 7, 52].

The weak measurement strategy enables an interesting and important LG test, since one can experimentally demonstrate (independently of the quantum prediction) the *noninvasiveness of the weak measurement*, by showing the invariance of $\langle S_1 S_3 \rangle$ as $\gamma \to 0$ when the measurement is performed at t_2. This implies a zero disturbance as $\gamma \to 0$

$$d_\sigma \equiv \langle S_3 | \hat{M}_2, \sigma \rangle - \langle S_3 | \sigma \rangle = 0 \quad (10)$$

where d_σ is defined in the Introduction. Different to the previous strategies, the *three* measurements can therefore be carried out in a *time-ordered sequence* for each given run: the preparation at time t_1, the weak measurement at time t_2, and the final projective measurement at t_3. This sequence yields for each run the values of the spin products $S_1 S_2$, $S_1 S_3$ and $S_2 S_3$ required for the LG inequality. The moments $\langle S_i S_j \rangle$ are evaluated by averaging over all runs. However, the weak measurement is not an actual measurement of S_2 (because it does not yield the value of S_2 being either $+1$ or -1) and one is surmising that the measured $\langle S_2 S_3 \rangle$ is that of the actual non-invasive measurement (NIM), which exists according to the LG premises.

Experiments that violate LG inequalities or else evaluate the moment $\langle S_2 S_3 \rangle$ using weak measurements have been carried out for systems of a single photon and for superconducting circuits. Violation of the LG inequality using this strategy is linked to the observation of quantum weak values and occurs only in the weak measurement limit where γ is small. The detailed study of quantum weak values for this system has been given in a different paper [22]. This strategy is useful where generalised NOON states are generated at time t_2, and where an INR measurement cannot be performed.

For γ sufficiently large, the weak measurement becomes a projective measurement, and the violation of the LG inequality is lost, if one uses the WM strategy of three successive measurements. This is clear, since the projective measurement will at any time yield the result of either 1 or -1, thus ensuring $LG \leq 1$. The Refs. [3, 22] calculate the threshold $\gamma > 0.52$ for the loss of the LG violation. For projective measurements, the violation of the LG inequality is achieved using the QND or INR approaches, where $\langle S_2 S_3 \rangle$ and/ or $\langle S_1 S_3 \rangle$ is inferred, based on the validity of the LG premises, as described in the previous Sections III.A and III.B.

The violation that is possible using projective measurements in one case (QND or INR strategies), but not the other (WM strategy), strengthens the argument for failure of the LG premises. The interpretation is that the projective measurement "collapses" the wave function at the time t_2, because, immediately prior to the measurement at time t_2, the system cannot be regarded as being in one state or the other. For systems where the quantum state at time t_2 can be shown to be in a classical mixture of the two states $|\psi_+\rangle$ and $|\psi_-\rangle$, this difference between the two cases does not occur, and there is no violation of the LG inequality.

IV. LG TESTS USING INTERFEROMETERS AND THE s-SCOPIC LG INEQUALITIES

LG tests can be carried out using a nonlinear or linear interferometer. This is depicted schematically in Figure 3a. Predictions for violations of Leggett-Garg inequalities using a linear interferometer are given in Figures 3b and c. Figures 2 and 4 shows violations using a nonlinear interferometer. In Figure 3a, the input state at time t_1 is a two-mode state with N bosons in one mode (implying $S_1 = 1$). The two-mode state undergoes a unitary transformation $BS1$ realised as either a beam splitter (with transmission intensity given by $\cos^2\theta$), or as the nonlinear beam splitter given by the nonlinear Josephson Hamiltonian H_I (Eq. (3)). After the interaction $BS1$, at time t_2, the sign S_2 of the mode population difference $\hat{J}_z$ may be measured, by the measurement we label $\hat{M}$. Subsequently, the two-mode system evolves according to a further unitary transformation. This is realised as a second nonlinear Josephson interaction H_I, or else as a second beam splitter (BS2, with transmission intensity given by $\cos^2\phi$). The unitary interaction $BS2$ may also be realised as a phase shift ϕ followed by a 50/50 beam splitter. At the output of the interferometer, the population difference $\hat{J}_z$ (and hence S_3) is measured at the final time t_3. A nonlinear interferometer of this type has been realised for atoms in the BEC experiments of Gross et al, based on the interaction H_I [37]. Figure 3b (solid blue and red dashed curves) plots predictions for LG tests in the linear case, where $H_I = 0$.

The LG inequalities might also be tested when mesoscopic superposition states are created at a time t_2 as heralded states, produced conditional on a certain outcome being obtained for a preparation measurement $\hat{P}$. For example, the macroscopic Hong-Ou-Mandel technique passes N bosons through a beam splitter $BS1$ (of transmission intensity $\cos^2\theta$) [26]. A QND measurement is made of $\hat{J}_z$ at the time t_0, and an output state $|\psi_\Delta\rangle$ is then heralded on the result J_z being $|J_z| > \Delta/2$ (here Δ is an integer, $\Delta < N$). This creates at t_2 a mesoscopic superposition

$$|\psi_\Delta\rangle = c_-|\psi_-\rangle + c_+|\psi_+\rangle \tag{11}$$

of two states $|\psi_+\rangle$ and $|\psi_-\rangle$ that are distinct by $\Delta+1$ (or more) particles in each arm of a two-mode interferometer [53]. Here $c_\pm$ are probability amplitudes. In this case, the time t_1 that is needed for the LG test is the time t_0, that of the preparation outcome $|J_z| > \Delta/2$. For the heralded state, this outcome is deterministic. Hence S_1 is specified $+1$ if the result of the measurement $\hat{P}$ is $|J_z| > \Delta/2$, and -1 otherwise. For the heralded state, S_1 is always $+1$. We note that for $\Delta = N-1$, the generalised NOON state (3) with $\theta = \tau$ is created at time t_2 using this method.

Figures 2, 3b, 3c and 4 show predictions for LG violations where a mesoscopic superposition $|\psi_\Delta\rangle$ (or a NOON state) has been created at time t_2, either by the conditional method or by the dynamics H_I. In Figures 2 and 4, it is supposed that subsequently, after the measurement

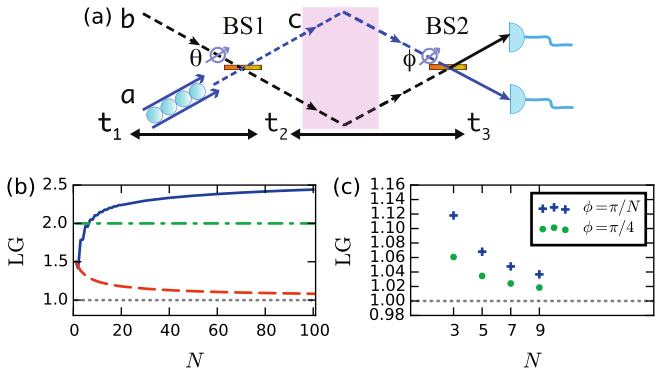

Figure 3. *LG tests using multiparticle interferometers:* In (a) N bosons pass through an interferometer. A measurement $\hat{M}$ (purple shading) is made on the state created at t_2 and the outgoing fields are combined across a beam splitter $BS2$ with transmission intensity $\cos^2\phi$. J_z of the outputs at time t_3 is measured. Plots (b) and (c) show results for the case of a simple linear interferometer where the bosonic modes are not coupled by the Josephson nonlinear interaction H_I. The blue solid curve and red dashed curve of (b) plot LG given by (1) for optimal angles θ, ϕ where the state at time t_2 is created by a simple beam splitter $BS1$ (transmission intensity $\cos^2\theta$). The red dashed curve of (b) shows LG for odd N where $\hat{M}$ is a non-clumsy measurement of S_2. The blue solid curve is where $\hat{M}$ measures $\hat{J}_z$ and hence the number of particles in arm c. This is a non-clumsy measurement of S_2 only when the number of particles in each arm is fixed. The green dotted-dashed curve shows the disturbance $d_\sigma = 2$ for optimal angles and N odd, where mesoscopic superposition states $|\psi_\Delta\rangle$ are created at t_2 by conditioning on $|J_Z| > \Delta/2$, as described in the text. Here $\hat{M}$ is a non-clumsy measurement of S_2. The green dotted-dashed curve shows the disturbance d_σ for all values of $\Delta \leq N-1$, including where a NOON state is created at t_2. Fig (c) shows LG where a NOON state is created at t_2, and where the final $BS2$ represents a phase shift ϕ and a 50/50 $BS2$ (for optimal $\tau = \theta$). Here $\hat{M}$ is a non-clumsy measurement of S_2.

$\hat{M}$, the system evolves according to the Josephson nonlinear interaction H_I. A measurement $\hat{J}_z$ is then made at t_3. This gives an LG test using a nonlinear interferometer. In Figures 3b (dotted-dashed green curve) and Figure 3c, it is supposed that between t_2 and t_3, $H_I = 0$, which corresponds to a linear interferometer.

With these different strategies, however, the outcomes for $\hat{J}_z$ at the times t_3 are not always restricted to $\pm N/2$ (Figure 4a). Before discussing the implications of the LG violations shown in Figures 2, 3 and 4, and to fully explore the possibilities for LG tests using interferometers, we address this case by deriving modified LG inequalities. To do this, we expand on previous work [2, 54].

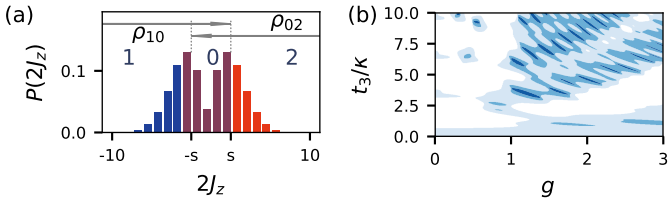

Figure 4. *Violation of s-scopic LG inequalities:* The NOON state (3) is created at time t_2 ($N = 5$, $\tau = \pi/6$) and evolves to time t_3 according to H_I with nonlinearity g. (a) Schematic of the probability distribution for results $2J_z$ at t_3. (b) Contours show regimes for violation of the s-scopic inequality (12) with $s = s_2 = s_3$, where (dark to light) $s = 4, 2, 0$.

A. The s-scopic LG inequalities

We consider a measurement $\hat{J}_z$ made on the system at time t_i and define three regions of outcome: region "1", $J_z < -s_i/2$; region "0", $-s_i/2 \leq J_z \leq s_i/2$; and region "2", $J_z > s_i/2$. Where the probability P_0 for a result in region 0 is zero, the regions 1 and 2 are distinct by s_i. The premise of *s_i-scopic realism* (s_iR) asserts that the system at time t_i (prior to measurement) is either in a state with an outcome in region "1", or in a state with outcome in region "2".

Generalising to $P_0 \neq 0$ (Fig. 4a), the meaning of s_iR is that the system at time t_i is in one or other of two *overlapping* states: the first that gives outcomes in regions "1" or "0" (denoted by $\tilde{S} = -1$); the second that gives outcomes in regions "0" or "2" (denoted by $\tilde{S} = 1$) [2, 54]. This premise adequately describes quantum superpositions of states that give outcomes of $\hat{J}_z$ different by up to s_i, but not (necessarily) superpositions of states with greater separations. The premise allows for an indeterminacy in the predetermination of the result of a measurement of $\hat{J}_z$ by an amount up to $\sim s_i$, since any such indeterminate state can be described as either $\tilde{S} = 1$ or $\tilde{S} = -1$. Macroscopic superpositions where there is the possibility of interpretation that the system would not comply with this restricted indeterminacy are not consistent with the premise. This approach was suggested originally by Leggett-Garg [2] and has been developed to provide tests of mesoscopic quantum coherence and mesoscopic Bell nonlocality [54, 55].

A measurement $\hat{J}_z$ gives the value of $\tilde{S}$ for regions 1 and 2, there being ambiguity only in the region 0. The second LG premise is generalised to *(s_2,s_3)-scopic noninvasive measurability* ((s_2, s_3)-NIM). This premise asserts that such a measurement can be made at t_2, without changing the result J_z at time t_3 by an amount s_3 or more. Any change or back-action due to the measurement by an amount up to s_3 will not alter the recorded value $\tilde{S}$ at time t_3, provided the experimenter takes into account that results in the region 0 cannot be distinguished as being either $\tilde{S} = +1$ or $\tilde{S} = -1$. Combined, we will refer to the s_iR and (s_2, s_3)-NIM premises as the s-scopic LG premises.

The s-scopic LG premises imply a quantifiable inequality, because any effects due to the ambiguous region are limited by the finite probability of observing a result there. Defining the measurable marginal probabilities of obtaining a result in region $j \in \{0, 1, 2\}$ at the time t_k by $P_j^{(k)}$, the s-scopic premises are violated if

$$LG_s \equiv P_2^{(2)} - P_1^{(2)} + \langle S_2 S_3 \rangle \\ -(P_2^{(3)} - P_1^{(3)}) - 2P_{0|M}^{(3)} - P_0^{(3)} > 1 \quad (12)$$

where $P_{j|M}^{(3)}$ ($P_j^{(3)}$) is the probability with (without) the measurement M performed at t_2. The details of the derivation are given in the Appendix A. We have assumed that the system is prepared initially in region 2 and restrict to scenarios satisfying $P_0^{(2)} = 0$. The $\langle S_2 S_3 \rangle$ is to be measured using a noninvasive measurement at t_2, as described in Section III. The $P_j^{(k)}$ are measurable by projective measurements. A similar modification can be given for the disturbance inequality.

B. Nonlinear interferometer

Figures 2 and 4b show violations of the s-scopic LG premises for nonzero s, using the nonlinear interaction H_I. Figure 2 is the nonlinear interferometer where the parameters N, g are selected to maintain a mesoscopic superposition throughout the evolution. Oscillations of this type have been realised in the experiments of Albiez et al based on BEC with Rb atoms [29]. A relevant measure of macroscopicity in this case is the mass difference given by sm_A (in each mode) of the two states forming the superposition, m_A being the mass of each atom. Figure 4b shows the violation of the s-scopic LG inequalities for smaller N, where the NOON state ($N = 5$) is created at time t_2, followed by evolution according to the nonlinear Hamiltonian H_I until time t_3. Here, the state created at t_3 need not be a NOON state, depending on the value of g.

C. Linear interferometer

LG tests are also possible where $H_I = 0$ (Figure 3). First we consider the simplest case depicted by the diagram Figure 3a, where an N-boson state at time t_2 is created by the simple beam splitter $BS1$ (transmission intensity $\cos^2\theta$), or equivalently a polariser beam splitter rotated at angle θ. Here, it is possible to test the hypothesis of individual classical trajectories for the bosons travelling through the linear interferometer.

The proposed experiment is as follows: After t_1, the N bosons pass through the polariser beam splitter (or equivalent) ($BS1$) rotated at angle θ. For the evaluation of $\langle S_2 S_3 \rangle$, a measurement $\hat{M}$ of J_z is made at time t_2. The number difference J_z indicates the value of J_θ (and

hence S_2) at t_2. The spin S_i is defined as in Section II at each time t_i to be the sign of J_z. The outgoing particles are then incident on a second polariser beam splitter $BS2$ at angle ϕ (or equivalently, a beam splitter with transmission intensity $\cos^2\phi$) whose output number difference J_z gives J_ϕ and hence S_3 at t_3. We invoke the LG premise, that the system is always in a state of definite J_z immediately prior to the measurement $\hat{M}$ at t_2. This is based on the hypothesis that *each* atom (boson) goes one way *or* the other, through the paths of the interferometer. A second LG premise is invoked, that a measurement $\hat{M}$ could be performed of J_z at t_2 that does not disturb the subsequent evolution. The second premise can be supported by experiments that create a spin eigenstate, and then demonstrate the invariance of the state after the QND number measurement $\hat{M}$. If the premises are valid, the LG inequalities (1) will hold, but by contrast are predicted violated by quantum mechanics (Fig. 3b (blue solid curve)). We assume fixed number inputs, achievable for photons [11] and likely in the future for atoms given the recent demonstration of quantum correlated atomic beams [27, 56].

We note that for this case the violation is given only for $s = 0$, and that NOON states are not created at the time t_2. While not the macroscopic LG envisaged, this nonetheless allows a test of the "classical trajectories" hypothesis that can be applied to atoms in a two-mode interferometer [37, 38, 49]. The violation of the LG inequality demonstrates the absence of individual classical trajectories, as in *each* atom passing through one arm or mode of the interferometer. Potential loopholes associated with the second premise are as for the QND measurement strategy, discussed in Section III.B and in the Conclusion, Section V. The details of the calculations are given in Appendix B, which includes a Table of the angles θ and ϕ required for the maximum violation.

The same experiment can be performed with a non-clumsy measurement (M) of S at time t_2. This corresponds to detecting the sign of the outcome for $\hat{J}_z$ at time t_2, without projecting the state into individual eigenstates of $\hat{J}_z$. Rather, the system after measurement is collapsed into the one of the states $|\psi\rangle_+$ or $|\psi_-\rangle$ which have a non-negative or negative outcome for $\hat{J}_z$ respectively. Such an experiment tests the following LG premises: the system is at any given time in one of the states $|\psi_+\rangle$ or $|\psi_-\rangle$ prior to measurement, and the measurement M does not influence the dynamics to the extent that the state of the system is changed from $|\psi_+\rangle$ to $|\psi_-\rangle$ (vice versa) at the time t_3. We see from the results plotted by the red dashed curve of Figure 3b that LG violations are possible (for $s = 0$). Here, the two states $|\psi_\pm\rangle$ are not mesoscopically distinct, except in the limit of $N \to \infty$ where the violation is vanishes ($LG \to 1$). Violations of s-scopic LG inequalities with $s > 0$ are not given in this case.

Where a NOON state is prepared at time t_2 and there is a spatial separation of the two trajectories at that time, stronger LG tests are possible. This is because the assumption of non-invasiveness of the measurement $\hat{M}$ at time t_2 can be strengthened by using an ideal negative result (INR) method (refer Section II). Violations of the Leggett-Garg inequality are shown for this case in Figs. 3b and c. The green dashed curve of Figure 3b shows $d_\sigma = 2$. This implies violation of the disturbance equality (2), where the mesoscopic superposition $|\psi_\Delta\rangle$ of Eqn. (11) is created at time t_2, and where the measurement at time t_3 is of J_ϕ, defined in the first paragraph of this Section. The detailed calculations are given in Appendix C. Similar violations are possible for the LG inequality (1), with the calculations also given in Appendix C. We see from those calculations that the violations of LG inequality (1) are enhanced where a NOON state is created at the time t_2, and increase with N, for odd N. Figure 3c shows violations of the LG inequality where a NOON state is created at time t_2, but where the measurement at time t_3 is replaced with the phase shift ϕ followed by a beam splitter. Violations are obtained with $s_2 = N$. All violations shown in Figure 3 are however for $s_3 = 0$. Details of the calculations are provided in Appendix D.

V. CONCLUSION

In this paper, we have developed strategies for tests of Leggett-Garg's mesoscopic realism using multi-particle interferometers, based on the nonlinear Josephson interaction model H_I. By deriving modified inequalities that apply where not all outcomes are mesoscopically distinct, we find the tests are enhanced over a wider range of parameter values. The interaction H_I is fundamental not only to Bose-Einstein condensates but describes Josephson effects in superconductors [45], superfluids [46] and, more recently, exciton polaritons [47]. We have also proposed tests of LG realism at a microscopic level, that apply to multi-particle linear interferometers where $H_I = 0$.

Finally, to conclude the paper, we summarise potential loopholes for the strategies outlined in this paper. For the ideal negative result (INR) and QND strategies given in Sections III.A and III.B, the violation of macro-realism arises because the value of $\langle S_1 S_3\rangle$ depends on whether the measurement $\hat{M}$ is made at time t_2. Specifically, the disturbance d_σ defined by Eq. (2) is nonzero. These tests are therefore only convincing when the measurement $\hat{M}$ that is used to evaluate the $\langle S_2 S_3\rangle$ can be justified as macroscopically non-invasive. The macro-realist, who believes the system is always in one of two macroscopically distinguishable states ψ_+ and ψ_-, will challenge this justification.

For the QND strategy of III.B, the non-invasiveness of $\hat{M}$ is justified by preparing the system in the states $\psi_\pm$ and demonstrating no-disturbance $d_\sigma = 0$ in each case. Assuming the quantum states $|\psi_\pm\rangle$ can be reliably prepared, this is a convincing demonstration that the system is not in one or other of quantum states $|\psi_\pm\rangle$ at the given time. The experiment thus demonstrates macroscopic quantum coherence: the system is not in a classical mix-

ture of the states $|\psi_\pm\rangle$. However, the macro-realist is not restricted to quantum mechanicsand would be ready to consider alternative descriptions of $\psi_\pm$ that are consistent with macro-realism. The macro-realist may argue that alternative (non-quantum) realisations of the states $\psi_\pm$ exist, the measurement $\hat{M}$ being invasive for such a realisation. A related loophole is the difficulty of preparing all realisations of the macroscopic state $\psi_\pm$, this being a manybody state for which there can be many microscopically different realisations possessing the same value for a macroscopic parameter. The macro-realist may also argue that the system at time t_2 is in a state *microscopically different* to either $|\psi_+\rangle$ or $|\psi_-\rangle$, the measurement $\hat{M}$ being microscopically invasive for this state (causing the collapse to $|\psi_+\rangle$ or $|\psi_-\rangle$). The microscopic change at time t_2 brought about by $\hat{M}$ may lead to a macroscopic change at time t_3, thus explaining the violation of the LG inequality in a way that is consistent with macro-realism. In short, the macro-realist would want to be convinced that the experimentalist can prepare all relevant quantum (and non-quantum) states for the test of non-clumsiness of the measurement.

The weak measurement (WM) strategy III.C has the advantage that justification of non-invasiveness is not required, the disturbance d_σ being zero. The $d_\sigma = 0$ is verifiable experimentally. There is no need to assume anything about the nature of the state at time t_2 to demonstrate the non-invasiveness. Rather, the test of macro-realism uses the LG inequality for 3 sequential measurements. The spins S_1, S_2 and S_3 are measured consecutively for each run, and the moment $\langle S_2 S_3\rangle$ is verifiable as that given by strong measurements. The macro-realist is left to argue that, being an ineffectual measurement of S_2 (that does not yield a value of $+1$ or -1 for a given run), the weak measurement is not the NIM implied by the LG premises.

In our view, the ideal negative result (INR) strategy given in III.A, based on a spatial separation of the modes, provides the strongest test of macro-realism. This strategy does not rely on the re-creation of the states $\psi_\pm$ for demonstrating non-invasiveness. Rather, the assumption of non-invasiveness is based on the assumption of locality. However, local realism has been shown to fail for microscopic systems and the macro-realist would likely argue that the measurement M does indeed cause a nonlocal *microscopic* change to the system at the second location. The macro-realist would argue that this microscopic change a time t_2 leads to a macroscopic change at time t_3, thus explaining the violation of the LG inequality in a way that is consistent with macro-realism. The realist's argument however relies on more macroscopic aspects of nonlocality for atomic systems that have not yet been verified.

ACKNOWLEDGMENTS

We thank P. Drummond and R.Y. Teh for stimulating discussions This research was supported by the Australian Research Council under grant DP140104584. This work as performed in part at the Aspen Center for Physics, which is supported by National Science Foundation grant PHY-1607611.

APPENDIX

Appendix A: Derivation of s-scopic LG inequalities

According to the premise sR, the system can be described by a model in which the system is in one of the states $\tilde{S} = -1$ or $\tilde{S} = +1$ at each t_i. We denote the probability of the system being in state $\tilde{S} = +1$ (-1) at a given time by $\tilde{P}_+$ $(\tilde{P}_-)$, noting that $\tilde{P}_+ + \tilde{P}_- = 1$. This defines a sequence of values $\tilde{S}_i$ such that the values are unchanged by the sNIM. Following the original derivation of LG inequality (1), this leads to $-3 \leq \tilde{S}_1\tilde{S}_2 + \tilde{S}_2\tilde{S}_3 - \tilde{S}_1\tilde{S}_3 \leq 1$. Thus, where $K_{ij} = \langle \tilde{S}_i\tilde{S}_j\rangle$, the inequality $K_{12} - K_{13} + K_{23} \leq 1$ of the form (1) holds.

However, the moments $\langle K_i K_j\rangle$ are not *directly* measurable, because an outcome between $-s/2$ and $+s/2$ could ambiguously arise from either state, $\tilde{S} = -1$ or $+1$. Regardless, $P_1 \leq \tilde{P}_- \leq P_1 + P_0$ and $P_2 \leq \tilde{P}_+ \leq P_2 + P_0$, where P_1, P_2 and P_0 are the measurable probabilities of obtaining a result for J_z in regions 1, 2 and 0 respectively. Hence, we are able to establish bounds on the two-time moments if the P_0 are measured. The modified inequality is

$$LG_s = K_{12}^{lower} + K_{23}^{lower} - K_{13}^{upper} \leq 1 \tag{A1}$$

Here K_{ij}^{lower} is a lower bound to K_{ij}, and K_{ij}^{upper} is an upper bound to K_{ij}. We see that suitable such bounds are given by $K_{ij}^{lower} = P_{2,2}(t_i,t_j)+P_{1,1}(t_i,t_j)-P_{10,20}(t_i,t_j)-P_{20,10}(t_i,t_j)$ and $K_{ij}^{upper} = P_{20,20}(t_i,t_j) + P_{10,10}(t_i,t_j) - P_{1,2}(t_i,t_j) - P_{2,1}(t_i,t_j)$. We introduce the notation that $P_{20,10}(t_1,t_2)$, for example, is the joint probability of an outcome J_z in regions 2 or 0 at time t_1, and an outcome of J_z in regions 1 or 0 at time t_2.

It is assumed that a measurement has been made of the moment $\langle S_2 S_3\rangle$ where S_j is determined by the sign of J_z at time t_j. For example, the moment $\langle S_2 S_3\rangle$ can be measured using a weak measurement at time t_2. Alternatively, the moment might be evaluated using the ideal negative result (INR) method. We wish to express the inequality (A1) in terms of this moment. We proceed by noting the following relations

$$\begin{aligned} K_{23}^{lower} &= \langle S_2 S_3\rangle - 2P_0^{(2)} - 2P_{0|M}^{(3)} \\ K_{13}^{upper} &= P_0^{(3)} + P_2^{(3)} - P_1^{(3)} \\ K_{12}^{lower} &= P_2^{(2)} - P_1^{(2)} - P_0^{(2)} \end{aligned} \tag{A2}$$

Here $P_j^{(k)}$ is the probability of an outcome for J_z in region j ($j = 0, 1, 2$) at the time t_k. We denote $P_{0|M}^{(3)}$ ($P_0^{(3)}$) as the probability for a result in the region 0 at t_3 if the measurement M is performed (or not performed) at t_2. We note that the $P_0^{(3)}$ and $P_{0|M}^{(3)}$ can be evaluated experimentally for a particular M. For the weak measurement as $\gamma \to 0$ the difference between $P_0^{(3)}$ and $P_{0|M}^{(3)}$ becomes zero.

Using the above results and the LG_S inequality defined by Eq. (A1), we obtain

$$\begin{aligned} LG_s \equiv & P_2^{(2)} - P_1^{(2)} - (P_2^{(3)} - P_1^{(3)}) \\ & + \langle S_2 S_3 \rangle - 3P_0^{(2)} - 2P_{0|M}^{(3)} - P_0^{(3)} \leq 1 \end{aligned} \quad \text{(A3)}$$

which reduces to Eq. (12) of the paper. The proof is given below.

Proof: First we prove $K_{23}^{lower} = \langle S_2 S_3 \rangle - 2P_0^{(2)} - 2P_0^{(3)}$. We note $K_{23} = P(+,+) + P(-,-) - P(+,-) - P(-,+)$ where $P(i,j)$ is the joint probability the system is in state i and j at times t_2 and t_3 respectively, and $+$ and $-$ are the states with $\tilde{S} = +1$ and -1. Hence

$$\begin{aligned} K_{23} = & P_{2,2} + P_{0|+,0|+} + P_{0|+,2} + P_{2,0|+} \\ & + P_{1,1} + P_{0|-,1} + P_{1,0|-} + P_{0|-,0|-} \\ & - P_{1,2} - P_{0|-,2} - P_{0|-,0|+} - P_{1,0|+} \\ & - P_{2,1} - P_{2,0|-} - P_{0|+,0|-} - P_{0|+,1} \end{aligned} \quad \text{(A4)}$$

Here $P_{2,2}$ is the joint probability for a result in region 2 at times t_2 and t_3. $P_{0|+,1}$ is the joint probability for an outcome at time t_1 in the region 0, given the system is in the state $+$ (at time t_1), and an outcome in region $+1$ at time t_3. The remaining probabilities are defined similarly. Defining $\langle S_2^+ S_3^+ \rangle = P_{2,2} + P_{1,1} - P_{1,2} - P_{2,1}$ and simplifying we obtain

$$\begin{aligned} K_{23} & \geq \langle S_2^+ S_3^+ \rangle - P_{0|-,2} - P_{0|-,0|+} - P_{1,0|+} - P_{2,0|-} \\ & \quad - P_{0|+,0|-} - P_{0|+,1} \\ & \geq \langle S_2^+ S_3^+ \rangle - P_{0|-}^{(2)} - P_{0|+}^{(2)} - P_{0|+}^{(3)} - P_{0|-}^{(3)} \\ & \geq \langle S_2^+ S_3^+ \rangle - P_0^{(2)} - P_0^{(3)} \end{aligned} \quad \text{(A5)}$$

Here $P_{0|(\pm)}^{(k)}$ is the probability for an outcome in the region 0 given the system is in the state $(\pm)$ at time t_k. $P_0^{(k)}$ is the probability for an outcome in region 0 at time t_k. Now we note that the measurable moment is

$$\begin{aligned} \langle S_2 S_3 \rangle = & P_{2,2} + P_{0+,0+} + P_{0+,2} + P_{2,0+} \\ & + P_{1,1} + P_{0-,1} + P_{1,0-} + P_{0-,0-} \\ & - P_{1,2} - P_{0-,2} - P_{0-,0+} - P_{1,0+} \\ & - P_{2,1} - P_{2,0-} - P_{0+,0-} - P_{0+,1} \end{aligned} \quad \text{(A6)}$$

where $P_{0+,0+}$ is the probability of a positive outcome in region 0 for both times. The other probabilities are defined similarly. Then we simplify

$$\begin{aligned} \langle S_2 S_3 \rangle = & \langle S_2^+ S_3^+ \rangle + P_{0+,0+} + P_{0+,2} + P_{2,0+} + P_{0-,1} \\ & + P_{1,0-} + P_{0-,0-} - P_{0-,2} - P_{0-,0+} - P_{1,0+} \\ & - P_{2,0-} - P_{0+,0-} - P_{0+,1} \\ \leq & \langle S_2^+ S_3^+ \rangle + P_{0+,0+} + P_{0+,2} + P_{2,0+} + P_{0-,1} \\ & + P_{1,0-} + P_{0-,0-} \\ \leq & \langle S_2^+ S_3^+ \rangle + P_{0+}^{(2)} + P_{0+}^{(3)} + P_{0-}^{(2)} + P_{0-}^{(3)} \\ \leq & \langle S_2^+ S_3^+ \rangle + P_0^{(2)} + P_0^{(3)} \end{aligned} \quad \text{(A7)}$$

Hence, we obtain the result $K_{23} \geq \langle S_2 S_3 \rangle - 2P_0^{(2)} - 2P_0^{(3)}$ where $P_0^{(k)}$ is the probability for an outcome in region 0 at time t_k. From this we obtain that $K_{23}^{lower} = \langle S_2 S_3 \rangle - 2P_0^{(2)} - 2P_{0|M}^{(3)}$ where we have inserted the $|M$ to remind us that the marginal probabilities for a result in the regions at time t_3 in this case are taken after the measurement M at time t_2.

We next consider K_{13}. Here we wish to prove that $K_{13}^{upper} = P_0^{(3)} + P_2^{(3)} - P_1^{(3)}$. This can be done using projective measurements. We see from above that $K_{ij}^{upper} = P_{20,20}(t_i, t_j) + P_{10,10}(t_i, t_j) - P_{1,2}(t_i, t_j) - P_{2,1}(t_i, t_j)$. Here $K_{13}^{upper} = P_{20,20}(t_1, t_3) + P_{10,10}(t_1, t_3) - P_{1,2}(t_1, t_3) - P_{2,1}(t_1, t_3)$ which reduces to

$$K_{13}^{upper} = P_0^{(3)} + P_2^{(3)} - P_1^{(3)} \quad \text{(A8)}$$

where we have used that the system at t_1 is initially prepared in region 2, so that $P_2^{(1)} = 1$. Here we infer that the measurement at time t_3 is made without the measurement M at t_2.

Similarly, we next consider K_{12}. We have from above that $K_{ij}^{lower} = P_{2,2}(t_i, t_j) + P_{1,1}(t_i, t_j) - P_{10,20}(t_i, t_j) - P_{20,10}(t_i, t_j)$ which implies $K_{12}^{lower} = P_{2,2}(t_1, t_2) + P_{1,1}(t_1, t_2) - P_{10,20}(t_1, t_2) - P_{20,10}(t_1, t_2)$ This reduces to

$$K_{12}^{lower} = P_2^{(2)} - P_1^{(2)} - P_0^{(2)} \quad \text{(A9)}$$

Thus, using the above results, and applying the LG_s inequality given in Eq. (A1) we obtain the required result (A3).

Appendix B: N bosons through a linear interferometer

We give details of the proposal of Figure 3a where results are shown by blue solid curve of Fig. 3b. In this case, there is no nonlinear Hamiltonian evolution. The particles travel through two successive polariser beam splitters (PBS). The first beam splitter is set at angle θ. A measurement can then be made of the two mode number difference, defined as

$$J_\theta(t_2) = (\hat{c}^\dagger \hat{c} - \hat{d}^\dagger \hat{d})/2 = J_Z \cos 2\theta + J_X \sin 2\theta \quad \text{(B1)}$$

The normalised $S_2 = J_\theta(t_2)/(N/2)$ gives the value of the Leggett-Garg observable S_2. The polariser beam splitter

measurement can be realised by different physical means, including using a polariser beam splitter (with phase shifts) followed by a photon difference measurement, or, for atom interferometers, as a Rabi rotation followed by an atom number difference measurement [37, 57, 58]. Here J_z and J_x are defined in terms of the initial modes $\hat{a}$ and $\hat{b}$ (e.g. $J_z = (\hat{a}^\dagger\hat{a} - \hat{b}^\dagger\hat{b})/2$) and the rotated operators are given by

$$\hat{c} = \hat{a}\cos\theta + \hat{b}\sin\theta$$
$$\hat{d} = -\hat{a}\sin\theta + \hat{b}\cos\theta \tag{B2}$$

The measurement M of the number difference $= (\hat{c}^\dagger\hat{c} - \hat{d}^\dagger\hat{d})/2$ is made at time t_2 after the rotation denoted by θ (achieved by the polariser beam splitter). In terms of the Leggett-Garg inequality, the rotation denoted by θ in the linear proposal plays the role of the evolution denoted by t_2 in the nonlinear proposal. A subsequent similar rotation (denoted ϕ) and number measurement at time t_3 gives the outcome $S_3 = J_\phi(t_2)/(N/2)$ as illustrated in Figure 3a.

We suppose the initial state is the two-mode number state $|N\rangle_a|0\rangle_b$. The output state at time t_2 after the first beam splitter with rotation θ is

$$|N\rangle_a|0\rangle_b \to \sum_{n=0}^{N} c_n|n\rangle_c|N-n\rangle_d \tag{B3}$$

where

$$c_n = \sqrt{\frac{N!}{n!(N-n)!}}\cos^n\theta(-\sin\theta)^{N-n} \tag{B4}$$

After the second beam splitter with rotation ϕ, the output state in the $\hat{e}$ and $\hat{f}$ modes is (assuming no measurement M is made at t_2)

$$|N\rangle_a|0\rangle_b \to \sum_{n=0}^{N} c_n \sum_{p=0}^{N} c_p^{(n)}|p\rangle_e|N-p\rangle_f \tag{B5}$$

where

$$c_p^{(n)} = \sum_{k=\max(0,p-n)}^{\min(N-n,p)} \frac{\sqrt{n!(N-n)!}\sqrt{(N-p)!}\sqrt{p!}}{(p-k)!(n-p+k)!k!(N-n-k)!} \times (-1)^{n-p+k}\left\{\cos^{(N-n+p-2k)}\phi\sin^{(n-p+2k)}\phi\right\} \tag{B6}$$

Calculation gives

$$\langle S_1S_2\rangle = \sum_{n=0}^{N} sgn\,(2n-N)\,c_n^2$$
$$\langle S_1S_3\rangle = \sum_{p=0}^{N} sgn\,(2p-N)\left(\sum_{n=0}^{N} c_n c_p^{(n)}\right)^2$$
$$\langle S_2S_3\rangle = \sum_{n=0}^{N} sgn\,(2n-N)\,c_n^2 \sum_{p=0}^{N} sgn(2p-N)\left(c_p^{(n)}\right)^2 \tag{B7}$$

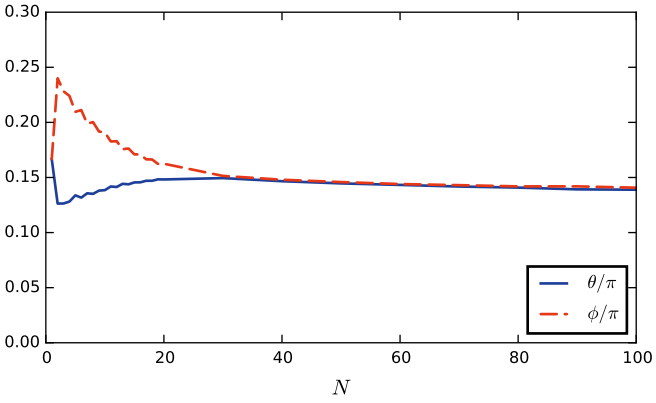

Figure 5. The optimal angles θ_{max} (solid blue line) and ϕ_{max} (dashed red line) that maximize the Leggett-Garg inequality for different values of N.

where $sgn(x) = 1$ if $x \geq 0$ and -1 of $x < 0$. The calculation of $\langle S_2S_3\rangle$ assumes the collapse of the wavefunction at time t_2 due to the projective measurement of J_z at t_2. The moment is then calculated as the weighted average of the individual moments based on all the possible projected eigenstates of J_z (number), which are then the initial states for the second polariser beam splitter.

Using the above results, we maximize the Leggett-Garg inequality violation and obtain the corresponding optimal angles θ_{max} and ϕ_{max}. Results are shown in Fig. 3b (blue solid curve) and Fig. (5).

To understand the nature of the LG violations in the linear case, we plot the probability distributions for the outcome J_z at the different times t. We assume the measurement of S is made as a QND measurement of J_z. The measurement if made at time t_2 thus collapses the state into the associated two-mode number state. For $N = 50$ the optimal angles are $\theta = 0.14518\pi$, $\phi = 0.14522\pi$. After the rotation $BS1$ with θ, the state created at time t_2 has the number distribution plotted in the top graph of Figure 6. This corresponds to $\langle S_1S_2\rangle = 1$. After the rotation with $\theta + \phi$, the state created at time t_3 has the number distribution plotted in the middle graph of Figure 6. This corresponds to $\langle S_2S_3\rangle = -0.927$. After the QND measurement at t_2, the resulting collapsed state is passed through the interferometer with angle ϕ. The number distributions at time t_3 for the three different collapsed states are plotted in the lower graph. Here we take the three most likely measurement results at time t_2 ($n = 41$ is the most likely, as shown in the top figure). The correlations for the three cases are: $n = 40$, $p(n) = 0.139022426845$, $\langle S_2S_3\rangle = 0.39867944914$; $n = 41$, $p(n) = 0.140876075688$, $\langle S_2S_3\rangle = 0.440046798966$; $n = 42$, $p(n) = 0.125419972345$, $\langle S_2S_3\rangle = 0.442832855968$. Here, $p(n)$ is the probability of the result n at the time t_2. The total correlation averaged over all outcomes is $\langle S_2S_3\rangle = 0.434$ and the LG violation is LG $= 2.361$.

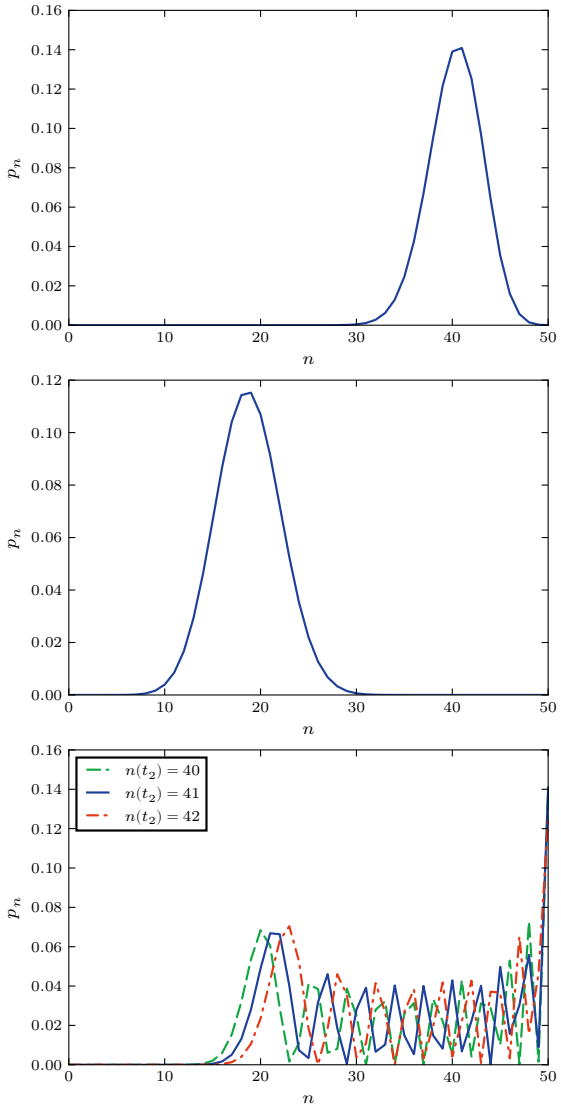

Figure 6. Plots of the probability distributions of number $n = J_z + N/2$ at the time t_2 (top), and at t_3 if a measurement is made at t_2 (lower) or if not (middle). Here $N = 50$ (the total particles in the interferometer), and n is the number of particles in one arm. The lower graph plots the distributions given that at time t_2 a QND measurement of n is performed with the outcome $n = 40$ (dashed green line), $n = 41$ (solid blue line) or $n = 42$ (dash-dotted red line).

Appendix C: Mesoscopic superposition at time t_2 in a linear interferometer

We suppose we create at time t_2 a superposition of two states $|\psi_+\rangle$ and $|\psi_-\rangle$ mesoscopically distinct (at time t_2), using, for example, a macroscopic Hong-Ou-Mandel effect. This effect uses a conditional measurement to create a mesoscopic superposition. We first evaluate the output state as created from the beam splitter $BS1$. We write the output state as a superposition $\psi = \sqrt{P_-}|\psi_-\rangle + \sqrt{P_0}|\psi_0\rangle + \sqrt{P_+}|\psi_+\rangle$ of three states defined by a positive parameter Δ that specifies a middle region of J_z of width Δ and centred about 0. Here $|\psi_\pm\rangle$ has outcomes J_z in region $J_z > \Delta/2$ and $J_z < -\Delta/2$ respectively, and $|\psi_0\rangle$ is a central state where outcomes for J_z satisfy $|J_z| \leq \Delta/2$. Here

$$|\psi_j\rangle = \frac{1}{\sqrt{P_j}} \sum_{n \in R_j(\Delta)} c_n |n\rangle_c |N-n\rangle_d \qquad \text{(C1)}$$

where $j \in \{-, +, 0\}$, $P_j = \sum_{n \in R_j} |c_n|^2$, and the regions are defined as $R_-(\Delta) = \{2n < N - \Delta\}$, $R_+(\Delta) = \{2n > N + \Delta\}$, $R_0(\Delta) = \{N - \Delta \leq 2n \leq N + \Delta\}$. The coefficients c_n are given in Eq. (B4). Before time t_2 (at a time we call t_1) a measurement is made that determines whether $|J_z|$ is in the central region or not. We assume this is a non-clumsy measurement, in the sense that the superposition state

$$|\psi_\Delta\rangle = \frac{1}{\sqrt{P_- + P_+}} (\sqrt{P_-}|\psi_-\rangle + \sqrt{P_+}|\psi_+\rangle) \qquad \text{(C2)}$$

is prepared at the time t_1, by conditioning the future evolution on an outcome $|J_z| > \Delta/2$ at time t_1. With this preparation, the result for S_1 is always 1. Note the time t_1 is defined differently to the above proposals, where the time t_1 refers to the preparation of N particles in the interferometer and no other conditional measurements are made.

a. *Evaluation of the LG inequality*

First, we evaluate

$$\langle S_1 S_2 \rangle = \frac{P_+ - P_-}{P_+ + P_-} \qquad \text{(C3)}$$

A second QND measurement of S_2 at time t_2 is made on the state $|\psi_\Delta\rangle$, to determine whether the system is in state $|\psi_+\rangle$ or state $|\psi_-\rangle$ (according to the LG premise). The non-clumsy QND measurement of S_2 corresponds to a QND measurement at t_2 that measures S_2 but does not resolve the precise number. To perform the calculation of $\langle S_2 S_3 \rangle$, we consider the system has collapsed to either $|\psi_+\rangle$ (if the result at t_2 is $S_2 = +1$) or $|\psi_-\rangle$ (if the result at t_2 is $S_2 = -1$). At time t_3 the outcome state for each of the functions $|\psi\rangle_\pm$ is given by

$$|\psi(t_3)\rangle_j = \sum_{n \in R_j(\Delta)} \frac{c_n}{\sqrt{P_j}} \sum_{p=0}^{N} c_p^{(n)} |p\rangle_e |N-p\rangle_f \qquad \text{(C4)}$$

Here the coefficients $c_p^{(n)}$ are given in Eq. (B6). Using these values we find

$$\begin{aligned} \langle S_2 S_3 \rangle &= \frac{P_+}{P_+ + P_-} \langle S_2 S_3 \rangle_+ + \frac{P_-}{P_+ + P_-} \langle S_2 S_3 \rangle_- \\ &= \frac{P_+}{P_+ + P_-} \langle S_3 \rangle_+ - \frac{P_-}{P_+ + P_-} \langle S_3 \rangle_- \end{aligned} \qquad \text{(C5)}$$

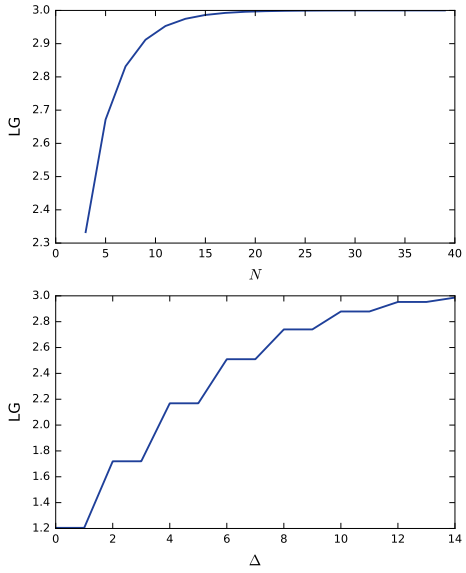

Figure 7. The top graph shows the violation of the LG inequality (1), as described in the text, for odd N and for the optimal choice of Δ and of the angles θ and ϕ. The optimal violation is achieved when the NOON state is created at time t_2. The lower graph shows the LG value for $N = 15$, versus Δ.

where $\langle S_3\rangle_\pm$ is the expectation value of S_3 at the time t_3 after the passage through the second $BS2$ set at angle ϕ, given the input state to the second beam splitter $BS2$ is $|\psi\rangle_\pm$. We note that

$$\langle S_2S_3\rangle = \frac{1}{P_+ + P_-}\left(\sum_{p=0}^{N}\Big(\sum_{n\in R_+(\Delta)} c_n c_p^{(n)}\Big)^2 - \sum_{p=0}^{N}\Big(\sum_{n\in R_-(\Delta)} c_n c_p^{(n)}\Big)^2\right)$$

Here $R_-(\Delta) = \{2n < N-\Delta\}$, $R_+(\Delta) = \{2n > N+\Delta\}$, $R_0(\Delta) = \{N-\Delta \le 2n \le N+\Delta\}$.

The moment $\langle S_1S_3\rangle$ is evaluated without the measurement S_2 at t_2, based on the superposition $|\psi_\Delta\rangle$ created at time t_1. This means we evaluate the expectation value of S_3 after a rotation given by beam splitter BS2 set at angle ϕ, for the full input state $|\psi_\Delta\rangle$.

The violation of the LG inequality (1) with no conditioning ($\Delta = 0$) is shown by the red dashed curve of Figure 3. The violations improve for non-zero Δ. Figure 7 shows the violation versus N for the optimal choices of angles θ and ϕ, and for the optimal value of $\Delta = N-1$. The violation is maximised by selecting $\Delta = N-1$ which corresponds to a NOON state at time t_2. The Table I shows the values, including the optimal angles, for the case $N = 11$. For $N = 15$, Figure 7 shows the violation versus Δ.

Δ	N	θ_{opt}	ϕ_{opt}	LG_{max}
1, 2	3	0.578973	0.495912	2.33291
1, 2	5	0.628767	0.33428	2.11778
1, 2	7	0.655977	0.254457	1.9855
1, 2	9	0.673675	0.206237	1.89226
1, 2	11	0.68629	0.17377	1.82165
1, 2	13	0.695819	0.150344	1.76568
3, 4	5	0.619339	0.475729	2.67167
3, 4	7	0.649188	0.356205	2.51489
3, 4	9	0.667305	0.287775	2.39912
3, 4	11	0.680023	0.24249	2.30743
3, 4	13	0.689619	0.210043	2.23205
5, 6	7	0.64078	0.465008	2.83173
5, 6	9	0.662639	0.36856	2.73091
5, 6	11	0.676442	0.3087	2.6466
5, 6	13	0.686464	0.266797	2.57372
7, 8	9	0.654105	0.458346	2.91181
7, 8	11	0.671783	0.376633	2.84982
7, 8	13	0.683173	0.323265	2.79288
9, 10	11	0.663216	0.45379	2.95311
9, 10	13	0.678323	0.382401	2.91581

Table I. Maximum values of the violation of the Leggett-Garg inequalities on optimising the choice of angles θ and ϕ, for fixed Δ and N.

b. *Evaluation of the disturbance inequality*

We now outline the calculation of the disturbance inequality. To evaluate $\langle S_3|\hat{M},\sigma\rangle$ we calculate the expectation of S_3 given that a projective (QND or INR) measurement is made at time t_2, with the state preparation at time t_1 as above for the macroscopic Hong-Ou-Mandel effect. Specifically

$$\begin{aligned}\langle S_3|\hat{M},\sigma\rangle &= \frac{P_+}{P_+ + P_-}\langle S_3\rangle_+ + \frac{P_-}{P_+ + P_-}\langle S_3\rangle_- \\ &= \frac{P_+}{P_+ + P_-}\langle S_2S_3\rangle_+ - \frac{P_-}{P_+ + P_-}\langle S_2S_3\rangle_-\end{aligned} \tag{C6}$$

where $\langle S_3\rangle_\pm$ are the expectation values for the states defined as $|\psi_\pm\rangle$. To evaluate $\langle S_3|\sigma\rangle$, we find the expectation of S_3 without the measurement at time t_2. From the calculations for the LG inequality

$$\langle S_3|\sigma\rangle = \langle\psi_\Delta|S_3|\psi_\Delta\rangle \tag{C7}$$

Applying the above results, we obtain that $d_\sigma = 2$ for $N = 3,\ldots,13$ and $\Delta = N-1$, using the values of the optimal angles. We also evaluate d_σ for $N = 13, 11$ and any value of Δ and we have obtained that $d_\sigma = 2$. The results are consistent with a violation of this inequality: $d_\sigma \neq 0$.

Appendix D: NOON state at time t_2 in a linear interferometer with phase shift

We consider where a NOON state is created at time t_2, either by dynamical evolution or using conditional methods as described above. The NOON state with spatially separated modes enables an ideal negative (INR) result measurement $\hat{M}$ at time t_2. In Fig 3c, we give results for the scheme where, after the measurement at time t_2, the system passes through the linear interferometer modelled by a phase shift ϕ followed by a 50/50 beam splitter. The transformations differ from the linear interferometer described above, which is based on a polariser beam splitter.

At time t_2 we suppose therefore that the state has evolved to a NOON state given by

$$|\psi(t_2)\rangle = \alpha|N\rangle_c|0\rangle_d + \beta|0\rangle_c|N\rangle_d \tag{D1}$$

where α and β are normalization coefficients. We take $\alpha = \cos\vartheta$ and $\beta = \sin\vartheta$. We note that the NOON state can in principle be prepared using the conditional approach described in Appendix B and in the text, in which case ϑ is determined by the beam splitter angle θ. We also comment that phase factors associated with β can change depending on the method of preparation, as seen on comparison with eq. (4). If necessary, such phase factors can be manipulated after the initial state preparation using phase shifts. At t_3 the output state is in $\hat{e}$ and $\hat{f}$ modes as given by

$$|\psi(t_3)\rangle = \frac{1}{\sqrt{2^N}}\sum_{m=0}^{N}\frac{\sqrt{N!}}{\sqrt{m!(N-m)!}} \times\left(\alpha+\beta e^{iN\phi}(-1)^{N-m}\right)|m\rangle_e|N-m\rangle_f \tag{D2}$$

The probability of detecting m photons at mode e and $N-m$ photons at d is

$$P_{m,N-m} = \frac{1}{2^N}\begin{pmatrix} N \\ m \end{pmatrix}\left(1+2\alpha\beta(-1)^{(N-m)}\cos(N\phi)\right) \tag{D3}$$

We obtain

$$\langle S_1S_2\rangle = \alpha^2-\beta^2 = \cos 2\vartheta$$
$$\langle S_1S_3\rangle = \sum_{m=0}^{N} sgn(2m-N)P_{m,N-m} \tag{D4}$$

For even N, $\langle S_1S_3\rangle = 0$. Noting that

$$\sum_{m=0}^{N} sgn\,(2m-N)\,\frac{1}{2^N}\begin{pmatrix} N \\ m \end{pmatrix}(-1)^{N-m} = X_N \tag{D5}$$

where

$$X_N = \frac{(-1)^{(N-1)/2}\,\Gamma\,(N/2)}{\sqrt{\pi}\Gamma\,((N+1)/2)}$$

N	LG_{max}	ϑ_{opt}	ϕ_{opt}
3	1.11803	-0.231824	$\pi/3$
5	1.068	0.179385	$\pi/5$
7	1.04769	-0.151442	$\pi/7$
9	1.03671	0.1333456	$\pi/9$
11	1.02984	-0.120649	$\pi/11$
13	1.02513	0.110936	$\pi/13$
15	1.0217	-0.103244	$\pi/15$
19	1.01705	-0.0916934	$\pi/19$
21	1.0154	0.0872034	$\pi/21$
51	1.00628	-0.0559035	$\pi/51$
101	1.00316	0.0397109	$\pi/101$

Table II. Maximum values of the violation of the Leggett-Garg inequalities on optimising the choice of angles ϑ and ϕ.

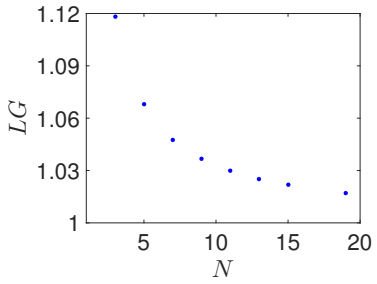

Figure 8. Violation of the Leggett-Garg inequality up to $N = 19$, for the optimal values of ϑ and ϕ as given in Table II.

we can simplify the correlation to (since $\alpha\beta = \frac{1}{2}\sin 2\vartheta$)

$$\langle S_1S_3\rangle = X_N \sin 2\vartheta\cos N\phi \tag{D6}$$

The final correlation is obtained by evaluating the weighted average where $|N\rangle|0\rangle$ and $|0\rangle|N\rangle$ are taken to be the initial state. This is based on the prediction for a non-clumsy projective measurement that collapses the state at time t_2, to either $|N\rangle|0\rangle$ or $|0\rangle|N\rangle$. Thus

$$\langle S_2S_3\rangle = \alpha^2\sum_{m=0}^{N} sgn(2m-N)\left|h^{(N)}\right|^2 -\beta^2\sum_{m=0}^{N} sgn(2m-N)\left|h^{(0)}\right|^2 \tag{D7}$$

where

$$h^{(N)} = \frac{1}{\sqrt{2^N}}\sqrt{\frac{N!}{m!(N-m)!}}$$
$$h^{(0)} = \frac{1}{\sqrt{2^N}}\sqrt{\frac{N!}{m!(N-m)!}}e^{iN\phi}(-1)^{N-m} \tag{D8}$$

We find that for all values of N, $\langle S_2S_3\rangle = 0$. For example

N	LG_{max}	ϑ_{opt}
3	1.06066	-0.169918
5	1.03456	0.1296
7	1.02412	0.108738
9	1.01852	-0.0954964
11	1.01503	-0.0861447
13	1.01264	0.0790904
15	1.01091	0.0735252
19	1.00856	-0.0652016
21	1.00773	0.0619757
51	1.00315	-0.0396122
101	1.00158	-18.8214

N	LG_{max}	ϑ_{opt}
3	1.08875	0.159386
5	1.0457	-0.107283
7	1.02943	0.0817553
9	1.02113	-0.0663958
11	1.01618	0.0560665
13	1.01295	-0.0486131
15	1.01068	0.0429661
19	1.00776	0.0349518
21	1.00877	0.139267
51	1.00622	-0.0610179
101	1.00302	0.031722

Table III. The Table on the left gives the maximum violation of the Leggett-Garg inequalities where ϑ is optimised at ϑ_{opt} for the fixed angle $\phi = \pi/4$. The Table on the right gives the maximum violation of the Leggett-Garg inequality where the angle ϑ is optimised at ϑ_{opt}, given the constraint $\phi = \vartheta$.

for $N = 3$

$$|3\rangle|0\rangle \to \frac{1}{\sqrt{8}}\left(|0\rangle|3\rangle + \sqrt{3}|1\rangle|2\rangle + \sqrt{3}|2\rangle|1\rangle + |3\rangle|0\rangle\right)$$
$$|0\rangle|3\rangle \to \frac{e^{i3\varphi}}{\sqrt{8}}\left(-|0\rangle|3\rangle + \sqrt{3}|1\rangle|2\rangle - \sqrt{3}|2\rangle|1\rangle + |3\rangle|0\rangle\right)$$

Hence

$$\langle S_2 S_3\rangle = \frac{\alpha^2}{8}(1+3-3-1) + \frac{\beta^2}{8}(1+3-3+1) = 0$$

For N even, there is no violation of the Leggett-Garg inequality (1) since $\langle S_2 S_3\rangle = 0$ and $\langle S_1 S_3\rangle = 0$. Thus the Leggett-Garg inequality for even N reduces to$LG = \langle S_1 S_2\rangle = \cos 2\vartheta < 1$. For odd N, the Leggett-Garg correlation is

$$LG = \cos 2\vartheta - X_N \sin 2\vartheta \cos N\phi \tag{D9}$$

It is possible to obtain violations of the Leggett-Garg inequality. The angles ϑ_{opt} and ϕ_{opt} that maximise the value of LG are

$$\vartheta_{opt} = \frac{1}{2}\arctan\left[X_N\right]$$
$$\phi_{opt} = \pi/N \tag{D10}$$

Substituting this into the expressions for $\langle S_1 S_2\rangle$ and $\langle S_1 S_3\rangle$, we obtain for the maximum value

$$LG = \sqrt{1 + X_N^2} \tag{D11}$$

Table II indicates the maximum violation as plotted in Figure 3c and the optimal values of ϕ and ϑ.

It is also possible to get violations of the Leggett-Garg inequality for fixed choice of angle ϕ. Here we select $\phi = \pi/4$ and find the optimal choice for ϑ is given by

$$\vartheta_{opt} = -\frac{1}{2}\arctan\left[X_N \cos\left(\frac{\pi N}{4}\right)\right] \tag{D12}$$

With these values we get the maximum violation

$$LG = \sqrt{1 + \frac{X_N^2}{2}} \tag{D13}$$

The corresponding values are given in the Table III. We also consider the case where $\vartheta = \phi$. Here, we obtain violations of the Leggett-Garg inequality for a suitable choice of ϕ as given in the Table III. The Figure 3c gives a summary of the violations of the Leggett-Garg inequality that are possible.

[1] E. Schroedinger, Naturwiss. **23**, 807 (1935).

[2] A. J. Leggett and A. Garg, Phys. Rev. Lett. **54**, 857 (1985).

[3] A. N. Jordan, A.N. Korotkov, and M. Buttiker, Phys. Rev. Lett. **97**, 026805 (2006).

[4] G. C. Knee et al., Nat. Commun. **7**, 13253 (2016).

[5] C. Li et al. Sci. Rep. **2**, 885 (2012). R. George et al, PNAS **110**, 3777 (2013). J. Kofler and C. Brukner, Phys. Rev. A **87**, 052115 (2013). L. Clemente and J. Kofler, Phys. Rev. A **91**, 062103 (2015). L. Clemente and J. Kofler, Phys. Rev. Lett. **116**, 150401 (2016). K. Wang et al., Phys. Rev. **95**, 032122 (2017).

[6] Emary, N. Lambert and F. Nori. Rep. Prog. Phys **77**, 016001 (2014).

[7] A. Palacios-Laloy et al., Nature Phys. **6,** 442 (2010).

[8] J. Dressel et al., Phys. Rev. Lett. **106**, 040402 (2011). J.S. Xu et al., Scientific Report **1**, 101 (2011).V. Athalye, S. S. Roy, and T. S. Mahesh, Phys. Rev. Lett. **107**, 130402 (2011). A. M. Souza, I. S. Oliveira and R. S. Sarthour, New J. Phys. **13** 053023 (2011). G. Waldherr et al., Phys. Rev. Lett. **107,** 090401 (2011). H. Katiyar et al., Phys. Rev. A **87**, 052102 (2013). R. E. George et al., Proc. Natl Acad. Sci. **110** 3777 (2013). C J. A. Formaggio et al., Phys. Rev. Lett. **117**, 050402 (2016). K. Wang et al., arXiv [quant-ph] 1701.02454. Z.-Q. Zhou et al., Phys. Rev. Lett. **115**, 113002 (2015).

[9] G. C. Knee et al., Nature Commun. **3**, 606 (2012).

[10] C. Robens, W. Alt, D. Meschede, C. Emary, and A. Alberti, Phys. Rev. X **5**, 011003 (2015).

[11] M. E. Goggin, et al., Proc. Natl. Acad. Sci. **108**, 1256 (2011).

[12] J. P. Groen et al., Phys. Rev. Lett. **111** 090506 (2013).

[13] Y. Suzuki, M. Iinuma and H. F. Hofmann, New J. Phys. **14**, 103022 (2012).

[14] H. Katiyar, A. Brodutch, D. Lu and R. Laflamme, New J. Phys, **19**, 023033 (2017)

[15] N. Lambert et al., Phys. Rev. A **94**, 012105 (2016).

[16] A. Asadian, C. Brukner and P. Rabl, Phys. Rev. Lett. **112**, 190402 (2014).

[17] C. Budroni et al., Phys. Rev. Lett. **115**, 200403 (2015). G. Vitagliano, presented at Workshop in Temporal Quantum Correlations and Steering, Siegen (2016).

[18] Y. Aharonov, D. Albert and L. Vaidmann, Phys. Rev. Lett. **60**, 1351 (1988). N. S. Williams, A. N. Jordan, Phys. Rev. Lett. **100**, 026804 (2008).

[19] G. J. Pryde, J. L. O'Brien, A. G. White, T. C. Ralph, and H. M. Wiseman. Phys. Rev. Lett. **94**, 220405 (2005).

[20] J. Dressel et al., Rev. Mod. Phys. **86**, 307 (2014).

[21] J. Dressel and A. N. Korotkov Phys. Rev. A **89**, 012125 (2014). T. C. White et al., NPJ Quantum Inf. **2,** 15022 (2016). B. L. Higgins et al., Phys. Rev. A **91**, 012113 (2015).

[22] L. Rosales-Zarate, B. Opanchuk and M. D. Reid, to be published Physical Review A.

[23] A. Leggett, Foundations of Physics **18**, 939 (1988). M. Wilde and A. Mizel, Foundations of Physics **42**, 256 (2011).

[24] G. C. Ghirardi, A. Rimini, and T. Weber, Phys. Rev. D **34**, 470 (1986). L. Diósi, Phys. Lett. A **120**, 377 (1987). R. Penrose, Gen. Relativ. Gravit. **28**, 581 (1996).

[25] J. P. Dowling, Contemporary Physics **49**, 125 (2008). I. Afek, O. Ambar, Y. Silberberg, Science **328**, 879 (2010). M. W. Mitchell, J. S. Lundeen and A. M. Steinberg, Nature **429**, 161 (2004). P. Walther et al., Nature **429**, 158 (2004).

[26] S. Slussarenko et al., Nature Photonics **11**, 700 (2017).

[27] R. Lopes et al., Nature **520**, 66 (2015). R. J. Lewis-Swan and K. V. Kheruntsyan, Nature Communications **5**, 3752 (2014).

[28] J. S. Bell, Physics **1,** 195 (1964).

[29] M. Albiez et al., Phys. Rev. Lett. **95** 010402 (2005).

[30] G. J. Milburn et al., Phys. Rev. A **55**, 4318 (1997). J. I. Cirac et al., Phys. Rev. A **57**, 1208 (1998). J. Dunningham and K. Burnett, Journ. Modern Optics, **48**, 1837, (2001). D. Gordon and C. M. Savage, Phys. Rev. A **59**, 4623, (1999). T. J. Haigh, A.J. Ferris, and M. K. Olsen, Opt. Commun. **283**, 3540 (2010).

[31] J. I. Cirac et al. , Phys. Rev. A **57**, 1208 (1998).

[32] Y. Zhou et al., Phys. Rev. A **67**, 043606 (2003).

[33] L. D. Carr, D. R. Dounas-Frazer, and M. A. Garcia-March, Europhys. Lett. **90,** 10005 (2010). D. R. Dounas-Frazer, A. M. Hermundstad and L. D. Carr, Phys. Rev. Lett. **99**, 200402 (2007).

[34] B. Opanchuk et al., Phys. Rev. A **94**, 062125 (2016). L. Rosales-Zarate, B. Opanchuk, Q. Y. He and M. D Reid, arXiv [quant-ph]:1612.05726.

[35] K. Pawlowski et al., Phys. Rev. **95**, 063609 (2017).

[36] J. Esteve et. al., Nature **455**, 1216 (2008).

[37] C. Gross et al., Nature **464** 1165 (2010).

[38] M. F. Riedel et al., Nature (London) **464**, 1170 (2010).

[39] N. Bar-Gill, C. Gross, I. Mazets, M. Oberthaler and G. Kurizki, Phys. Rev. Lett. **106**, 120404 (2011). Q. Y. He, M. D. Reid, T. G. Vaughan, C. Gross, M. Oberthaler and P. D. Drummond, Phys. Rev. Lett. **106**, 120405 (2011).

[40] K. Lange, J. Peise, B. Lücke, I. Kruse, G. Vitagliano, I. Apellaniz, M. Kleinmann, G. Tóth and C. Klempt, arXiv:1708.02480.

[41] P. Kunkel, M. Prüfer, H. Strobel, D. Linnemann, A. Frölian, T. Gasenzer, M. Gärttner and M. K. Oberthaler, arXiv:1708.02407. M. Fadel, T. Zibold, B. Décamps, P. Treutlein, arXiv:1708.02534.

[42] Q. Y. He et al., Phys. Rev. A **86**, 023626 (2012). B. Opanchuk et al., Phys. Rev. A **86**, 023625 (2012).

[43] D. Alcala, J. Glick and L. Carr, Phys. Rev. Lett. **118**, 210403 (2017).

[44] M. Steel and M. J. Collett, Phys. Rev. A **57**, 2920 (1998). H. J. Lipkin, N. Meshkov and A. J. Glick, Nucl. Phys. **62** 188 (1965).

[45] K. K. Likharev, Rev. Mod. Phys. **51**, 101 (1979). C. Wang et al., Science **352**, 1087 (2016). S. Zeytinoglu et al., Phys. Rev. A **91**, 043846 (2015). C. Eichler et al., Phys. Rev. Lett., **113**, 11502 (2014).

[46] S. Backhaus et al., Nature **392**, 687 (1998).

[47] M. Abbarchi et al, Nature Physics **9**, 275 (2013).

[48] D. Ananikian and T. Bergeman, Phys. Rev. A **73**, 013604 (2006).

[49] M. Egorov, et al., Phys. Rev. A **84**, 021605(R) (2011).

[50] O. Maroney and C. Timpson, (2014), arXiv:1412.6139v1

[51] E. O. Ilo-Okeke and T. Byrnes, Phys. Rev. Lett. **112**, 233602 (2014). J. Hope and J. D. Close, Phys. Rev. Lett. **93**, 180402 (2004).

[52] A. Chantasri, J. Dressel, and A. N. Jordan, Phys. Rev. A, **88**, 042110 (2013). J. F. Ralph, K. Jacobs and M. J. Everitt, Phys. Rev. A**95**, 012135 (2017). J. K. Eastman, J. Hope and A. R. Carvalho, Sci. Rep. **7**, 44684 (2017).

[53] M. Stobinska et al., Phys. Rev. A **86** 063823 (2012). T. Sh. Iskhakov et al., New J. Phys. **15**, 093036 (2013). K. Yu et al. , New J. Phys. **16**, 013025 (2014). G. J. Pryde and A. G. White, Phys. Rev. A **68**, 052315 (2003). A. E. B. Nielsen and K. Mølmer, Phys. Rev. A **75**, 063803 (2007).

[54] E. G. Cavalcanti and M. D. Reid, Phys. Rev. Lett. **97**, 170405 (2006); Phys. Rev. A. **77**, 062108 (2008). C. Marquardt et al., Phys. Rev. A **76**, 030101R (2007).

[55] M. D. Reid, to be published Physical Review A.

[56] R. I. Khakimov et al., Nature **540**, 100 (2016). C. Gross et al., Nature **480**, 219 (2011).

[57] T. Kovachy et al., Nature **528**, 530 (2015).

[58] K. S. Hardman et al., Opt. Lett. **41**, 2505 (2016).